

N79-19039

Paper No. 31

**APPLICATION OF AN ELECTRON BEAM FACILITY FOR
HEAT TRANSFER MEASUREMENTS IN CAPILLARY TUBES**

A. R. Lunde and Ted Kramer, *Boeing Aerospace Company, Seattle,
Washington*

ABSTRACT

A unique method has been developed for the determination of heat transfer coefficients for water flowing through capillary tubes using a rastered electron beam heater. Heat flux levels of 150 and 500 watts/cm² were provided on the top surface of four square tubes. Temperature gradient along the tube length and mass flow rates versus pressure drop were measured.

INTRODUCTION

The objective of this investigation was to provide the information necessary to design a convectively cooled foil window for a high power electron beam gun. A total of three test specimens were fabricated and tested. Testing was performed in the vacuum chamber of an electron beam facility. This facility was developed to provide a capability for vacuum testing materials and heat transfer systems which are exposed to high heat fluxes. The heat flux characteristics of this facility are shown in Figure 1. It can be seen that the range of test conditions extends from approximately 150 w/cm² on a 103 cm² area to over 10,000 w/cm² on an area of 1.5 cm².

The test facility is described herein. Descriptions of test articles and test setup are presented and details of heat flux calibration are given. Typical pressure drop and heat transfer results are reported and the results of burnout testing are shown.

ELECTRON BEAM HEATER

The Alloyd manufactured Electron Beam Heater, shown in Figure 2, consists of the electron gun, 15 KW cathode power supply, a 45 cm diameter by 75 cm vacuum chamber, and a 1500 liter/sec. diffusion pumping system. The electron gun is magnetically focused and deflected, and employs bias cup grid control of beam current. An accelerating anode effectively makes operation of the gun

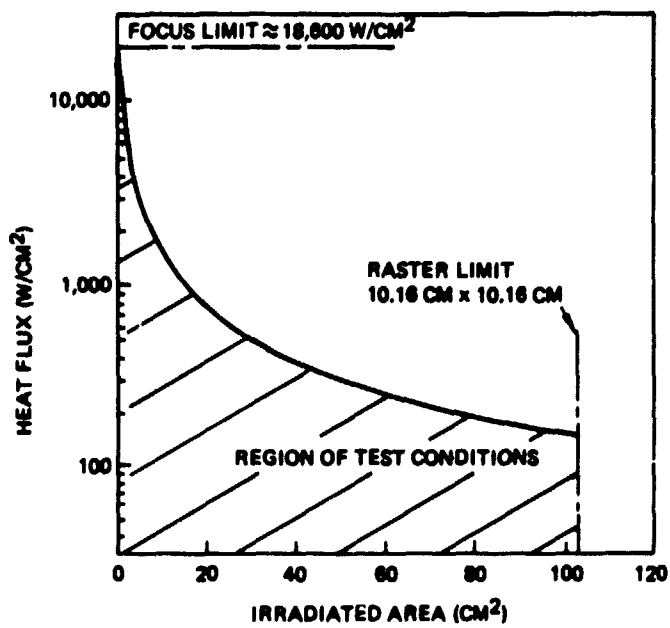


FIGURE 1 TEST CONDITION RANGE

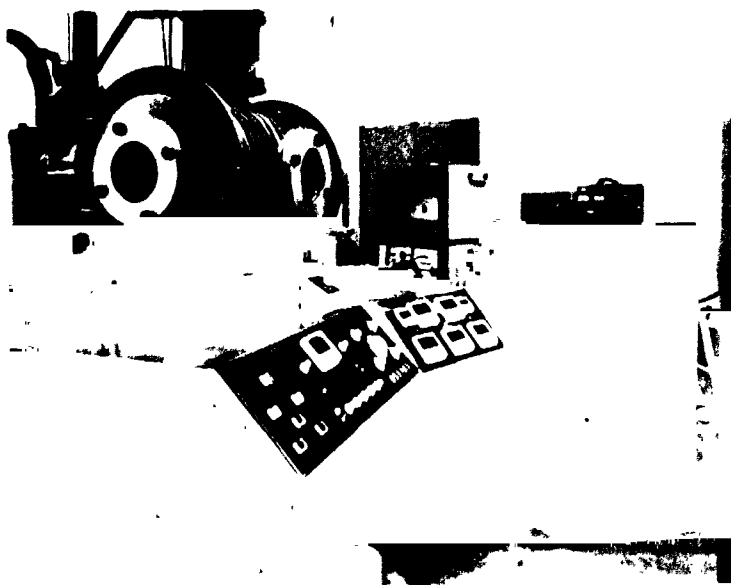


FIGURE 2 E-BEAM TEST FACILITY

independent of target geometry, spacing, and materials. The anode is connected to the system ground, thus focusing operation of the cathode and bias cup structures at high negative potentials. The tantalum ribbon filament cathode is directly heated by 20 to 30 amperes of current from a filament transformer.

The cathode power is provided unfiltered from a three-phase, full wave selenium rectifier bank and three-phase high voltage transformer. Power to the high voltage transformer is varied by a motor driven, three-phase variable auto-transformer connected to the 480 volt line. The auto-transformer drive motor is actuated in either direction by pushbuttons on the control panel.

A symmetrical two-axis stator-wound deflection coil was fabricated and fastened to a mount on the end of the original focus and deflection assembly. Deflection rates up to 120 kilocycles per second were verified. Two identical triangle-wave-form oscillators, power supply, and direct coupled driver amplifiers were designed and built with sweep rates from 10 cps to 100,000 cps. The dynamic deflection system is used for rectangular uniform raster production.

The vacuum system, employing an NRS-HS-6-1500 six inch diffusion pump and a Welch 1397 mechanical pump, is semi-automatic in operation, requiring only pushbutton actuation of all pumps and valves. Interlocks are provided to reduce probability of damage. Pump-down time starting with a hot diffusion pump is approximately 10 minutes.

TEST ARTICLE

A total of three test specimens were fabricated and tested. Each specimen consisted of four parallel water-cooled tubes. The tubes were square in cross section, measuring 0.0635 cm by 0.0635 cm outside dimensions with 0.00889 cm wall thickness. Tube material was 7075 T6 aluminum. The tubes terminated in manifolds instrumented with pressure taps. Tube span between manifolds was approximately 25 cm. The manifolds were supported on a common rigid plate with a support rib located beneath the tubes. The tubes were bonded to phenolic spacer blocks which were, in turn, bonded to the rib to provide dimensional stability during cyclic heating and cooling. Figure 3 shows specimens 1 and 2 which were identical in configuration. The coolant tubes were mounted side by side in these two specimens. The third test specimen was identical to the first two except the coolant tubes were spaced 0.23 cm between centerlines and a 1 mil aluminum foil was bonded with Mithra 200 epoxy to the top surface of the tubes. Figure 4 shows the foil configuration and tube arrangement of the third test specimen.



FIGURE 3 TEST SPECIMEN 1 & 2 CONFIGURATION

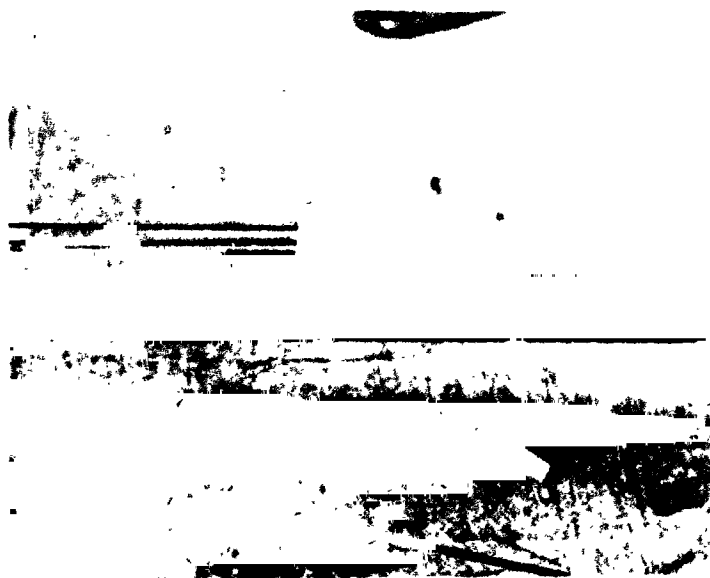


FIGURE 4 TEST SPECIMEN 3

Thermocouples of butt-welded 0.00508 cm chromel-constantan wire were bonded to the underside of the tubes at 2.5 cm increments along the length of the test section. Thermocouples were also bonded to the underside of the foil at a number of axial stations midway between the tubes of specimen three. Additional thermocouples were located on the water lines serving the inlet and outlet manifolds of all test specimens.

TEST CONFIGURATION

The test article was mounted in the vacuum chamber as shown in Figure 5. Water cooled shield plates were aligned along the length of the square tubes to shield the thermocouple leads. A reference calorimeter (Hy-Cal Model C-1312) was mounted adjacent to the test tubes within one of the shield plates. This allowed electron beam flux level to be established prior to irradiating the test tubes. Once irradiance level was established, the electron beam was rastered on to the test tubes for a specific time and then back to the reference calorimeter.



FIGURE 5 TEST ARTICLE MOUNTED IN CHAMBER

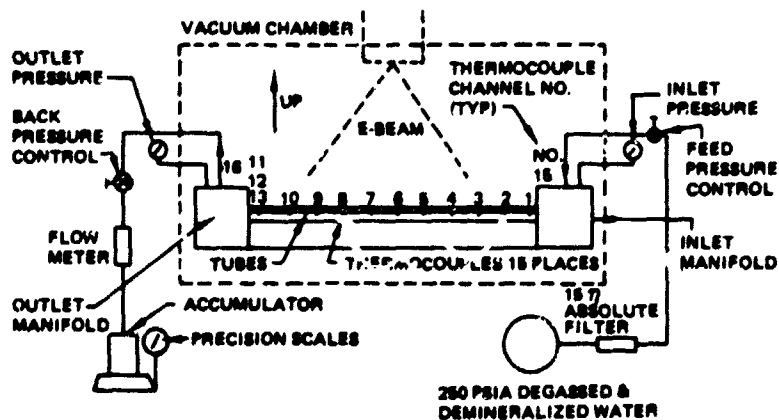


FIGURE 6 TEST SETUP SCHEMATIC

A schematic diagram of the test setup is shown in Figure 6. The test fluid was degassed, demineralized water. Flow rate was controlled by a valve ahead of the test specimen. A downstream valve was used to hold exit pressure to 4.65 atm. Pressure gauges connected to the inlet and outlet manifolds provided a rough reading of pressure drop and were used to set the inlet control valve. An electronic differential pressure transducer was connected across the manifold pressure tap lines for accurate pressure drop measurement.

Thermocouple voltage and pressure transducer signal were recorded continuously on magnetic tape. In addition, selected thermocouple signals and pressure drop were recorded on pen recorders to provide visual information required to monitor the experiment.

CALIBRATION PROCEDURE

Water flow rate versus pressure drop across the test specimen was determined prior to exposure to the electron beam. This was accomplished by starting with the maximum water pressure and maintaining a constant back pressure. The water flow rate passing through the test specimen was maintained for a given time, accumulated in a beaker and weighed. The supply pressure was then reduced for another set of conditions. This was continued down to a supply and back pressure difference of $3.45 \times 10^4 \text{ Kg/m-sec}^2$.

ORIGINAL PAGE IS
OF POOR QUALITY

Electron beam irradiance level and uniformity were measured prior to each test. This was accomplished by removing the test specimen and replacing it with a calibration assembly consisting of a Hy-Cal Model C-1312 S/N 36008 water cooled calorimeter mounted on a translating mechanism. Calorimeter response sensitivity was 0.0112 mv/(w/cm²).

The calibration assembly was designed so that the translating calorimeter could be moved along the test specimen axis. Care was taken to ensure that the elevation and coordinates of the calorimeter and test specimen were identical. At the beginning of each calibration, the calorimeter was centered at midspan. The chamber was pumped down and the electron beam established and shaped to give a line source approximately 0.60 cm wide by 12.7 cm long. Heater power was set to provide the desired midspan flux level. The calorimeter was then moved to a series of selected positions along the line source axis and the output recorded to establish the centerline beam irradiance levels. The calorimeter was repositioned at midspan and the electron beam line source offset 0.127 cm to the right and the measuring process repeated. This procedure was then repeated with the electron beam offset 0.127 cm to the left. At the completion of calibration the beam was rastered over to the reference calorimeter and its output recorded. The scanner assembly was then removed and the test specimen installed.

Figure 7 shows a typical set of irradiance scans. The centerline profile is seen to be relatively uniform along the scan axis; however, the profile for the 0.127 cm left-offset increases from left to right while the 0.127 cm right-offset profile decreases. This phenomenon was caused by the electron beam line source being slightly skewed relative to the direction of travel of the calorimeter. Since the scan axis and test section axis were coincident, the line source was skewed relative to the test section axis by an identical amount.

Analysis of heat transfer test results required a knowledge of the local flux intensity levels over the entire 0.40 cm wide by 12.7 cm long line source. The electron flux scans shown in Figure 7 were used to provide this information. It was assumed that the flux intensity in a plane perpendicular to the line source was normally distributed about the source axis as shown in Figure 8. Local offset of the line source axis and calorimeter centerline is L and the skew angle is θ . Electron flux intensity q was assumed to be a function of x , the distance from the line source centerline.

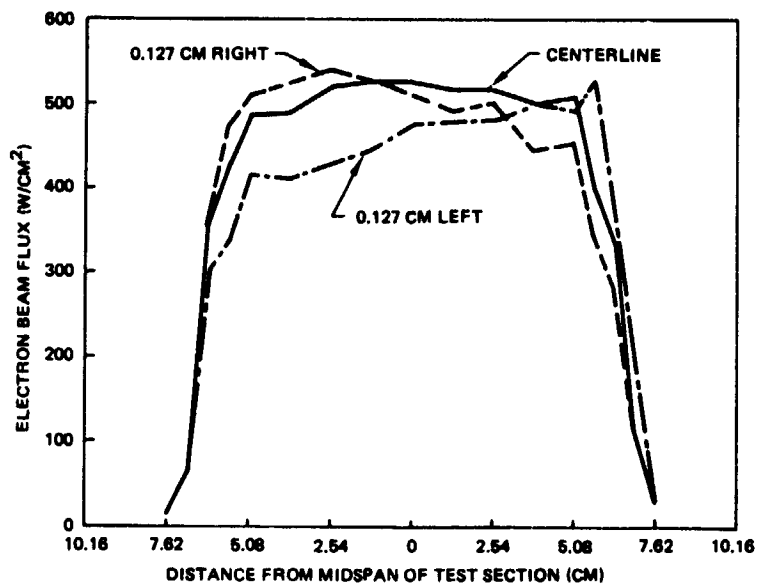


FIGURE 7 MEASURED FLUX ALONG TEST SECTION

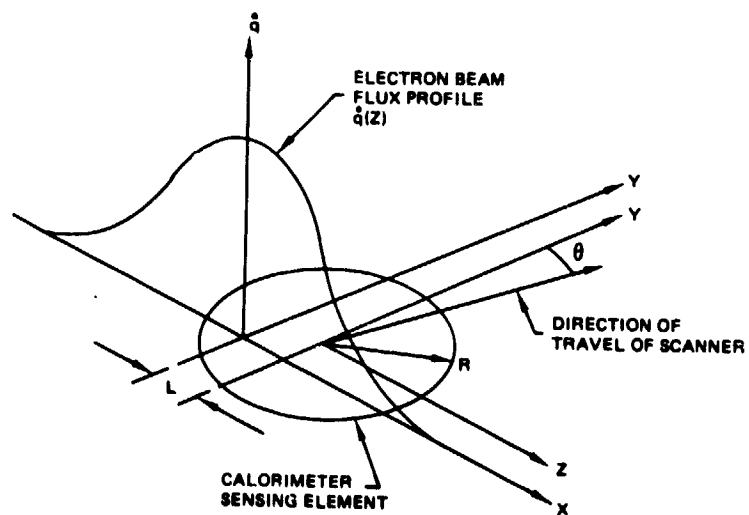


FIGURE 8 CALORIMETER & E-BEAM COORDINATES

The total amount of power Q incident on the 0.254 cm diameter calorimeter sensor was expressed as

$$Q = \int_{-R}^R \int_{-y}^y q(x) dy dz \quad (1)$$

where R = sensor radius

z, y = cartesian coordinates with origin at center of calorimeter sensor

Integrating in the y direction and introducing the relationship between radial location on the sensor and the cartesian coordinates z and y gave

$$Q = 2 \int_{-R}^R q(x) \sqrt{r^2 - z^2} dz \quad (2)$$

where $y = R^2 - z^2$

Since z and x were related by the expression

$$z = x + L \quad (3)$$

and q was assumed to be normally distributed, the expression for power incident on the calorimeter sensor became

$$Q = 2a \int_{-(R+L)}^{R-L} e^{-bx^2} \sqrt{R^2 - (x+L)^2} dx \quad (4)$$

For the case in which the beam was offset to the right by 0.127 cm, the expression for power delivered to the sensor was

$$Q' = 2a \int_{-(R+L+0.127)}^{(R-L-0.127)} e^{-bx^2} \sqrt{R^2 - (x+L+0.127)^2} dx \quad (5)$$

A similar expression was written for the case in which the beam was offset 0.127 cm to the left. This expression along with equations 4 and 5 represented three simultaneous equations which were solved for the unknowns a, b, and L.

Total incident power Q on the calorimeter sensor was calculated from electron beam flux scan data using the expression

$$Q = \pi R^2 q_m$$

where q_m = electron flux indicated by calorimeter

Figure 9 shows a typical calculated flux profile at one axial station. Measured data are spotted on the chart for comparison.

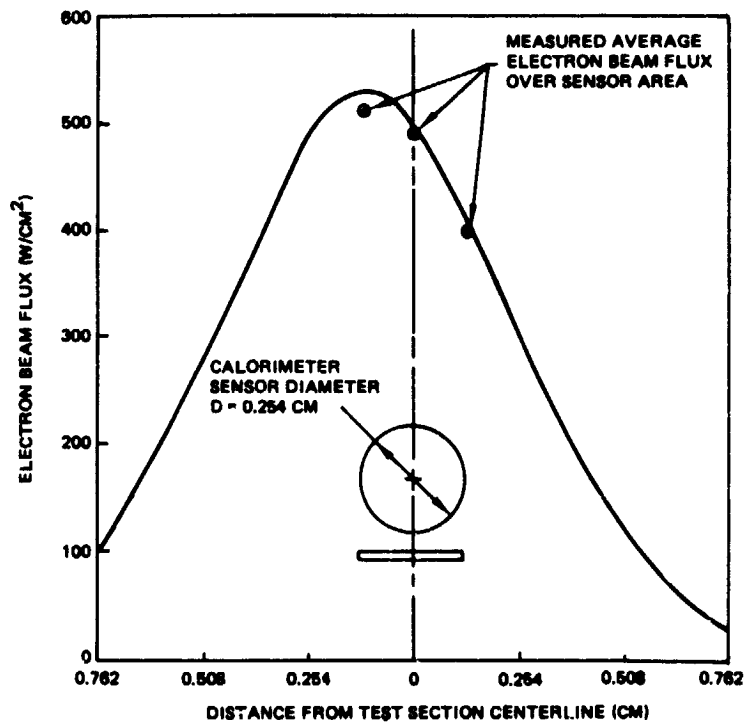


FIGURE 9 CALCULATED FLUX PROFILE

TEST PROCEDURE

The test chamber was pumped down and the electron-beam turned on to the reference calorimeter. The flux level was established as determined during calibration. The maximum water flow rate was established through the test

specimen and the temperature data acquisition initiated. Then, at a determined time, the electron beam was rastered over to the test specimen for a specific time interval and back to the reference calorimeter. The flow rate was decreased and the same procedure followed. Temperature, time, pressure difference, and water flow rate were recorded for a series of ranges of differential pressure from 3.45×10^4 Kg/m-sec² to 68.9×10^4 Kg/m-sec².

TEST RESULTS

Figure 10 shows measured mass flow rate as a function of friction pressure drop between the inlet and outlet manifolds of the test specimen. Friction pressure drop was calculated by subtracting dynamic loss from measured total pressure drop between manifolds. The tube entrance region loss was approximately 3% of the total pressure differential.

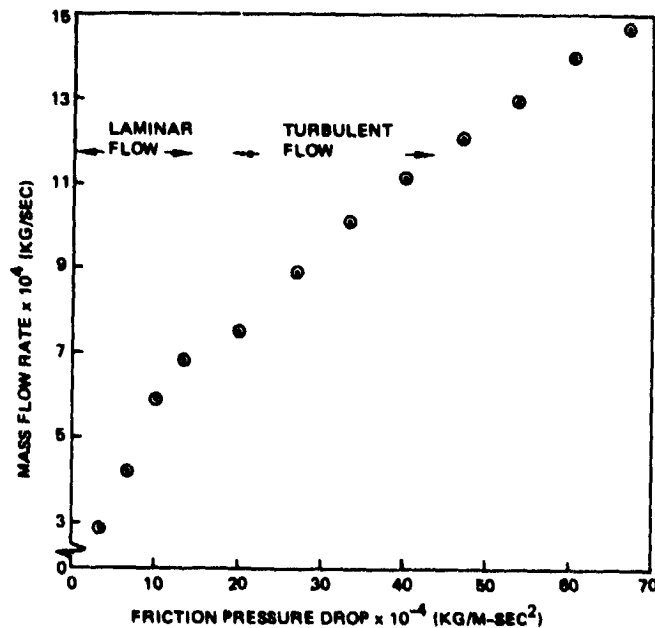


FIGURE 10 MASS FLOW RATE MEASUREMENTS

Typical measured wall temperatures along the tubes are shown in Figure 11. Electron beam flux level was 250 w/cm^2 for these results. Average convective heat transfer coefficients were calculated from measured tube wall temperatures with the aid of a computer routine which analyzed the combined convection/conduction heat

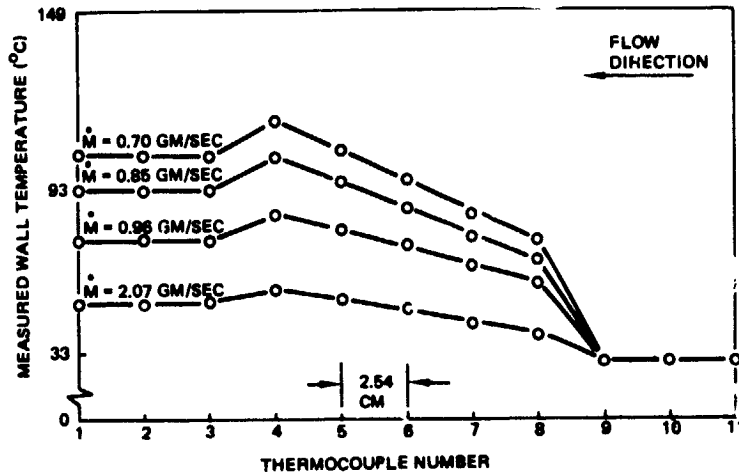


FIGURE 11 MEASURED TUBE WALL TEMPERATURES

transfer in the test section. A comparison of computed log-mean heat transfer coefficients with the classical correlation for heat transfer in round ducts is shown in Figure 12. The experimentally based results are seen to fall 10 to 16 percent below the round tube correlation for large flow channels. A complete description of the computer analysis and fluid flow and heat transfer results is presented in Reference 1.

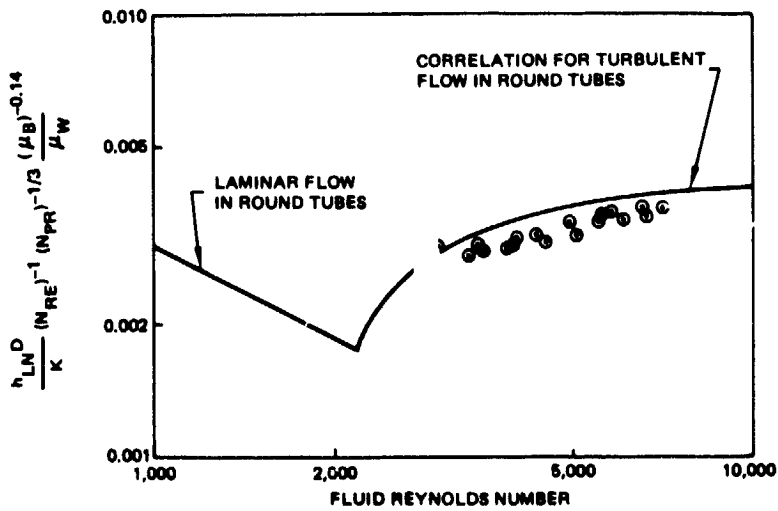


FIGURE 12 COMPARISON OF EXPERIMENTAL LOG-MEAN HEAT TRANSFER COEFFICIENTS WITH THE CLASSICAL CORRELATION

Testing was extended to burnout for all three specimens. Figure 13 shows tube burnout which occurred at a flow rate of 0.521 gm/sec. and a pressure drop of 6.9×10^4 Kg/m-sec². Electron beam flux at burnout was 204 w/cm². Failure was due to formation of vapor bubbles along the heated wall which drastically reduced the local convective heat transfer coefficient.

Figure 14 shows the results of foil burnout on specimen 3 which occurred at an electron flux of 150 w/cm². Failure was caused by low thermal conductance across the bond joint between foil and tubes. It was found that bond thickness could not be controlled with sufficient accuracy during application of the foil to the tubes so that a thickness limit of less than 0.00254 cm could not be maintained. In addition, it was not possible to test the bond joint for voids which would have contributed to its apparent high thermal resistance.

COMMENTS

The thermal bond between foil and coolant tubes represents the greatest resistance to heat flow in an electron beam foil window. Adhesive bonding does not provide sufficient joint conductance to support a foil heat deposition rate of 150 w/cm².

CONCLUSIONS

The electron beam facility utilizing a rastered electron beam heater is a flexible tool for vacuum testing materials and high heat flux cooling systems. Potential applications for this facility include testing space materials and components subjected to simulated laser heating, simulation of heating in radioisotope heat sources, and simulation of heating in rocket chambers and electronic components such as field effect transistors and RF generators.

Uniform heating can be achieved with the rastered electron beam. The heat flux field can be mapped with a water-cooled calorimeter.

Small thin-wall tubes are capable of supporting heat fluxes in excess of 500 w/cm² at moderate coolant pressure drops. Coolant flow rates must be maintained high enough that maximum tube wall temperature does not exceed the local saturation pressure of the coolant.



FIGURE 13 TUBE BURNOUT - SPECIMEN 1

ORIGINAL PAGE IS
OF POOR QUALITY

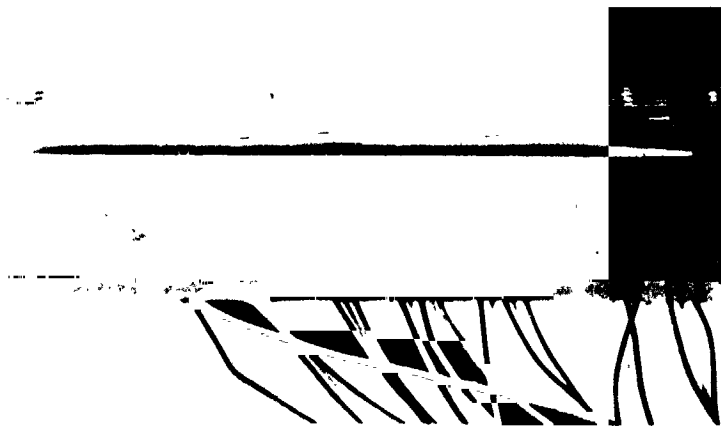


FIGURE 14 RESULTS OF FOIL BURNOUT

REFERENCES

- 1) Kramer, T. J., "Fluid Flow and Convective Heat Transfer in Square Capillary Ducts Subjected to Nonuniform High Heat Flux", ASME Paper No. 76-WA/HT-29, 1976.